Progress In Electromagnetics Research C, Vol. 173, 293–298, 2026 PIER C

(Received 22 June 2026, Accepted 9 September 2026, Scheduled 19 September 2026)

Power Divider Based on Broadside-Coupled Coplanar Waveguides

Young Kim*

School of Electronic Engineering, Kumoh National Institute of Technology, 61 Daehak-ro, Gumi, Gyungbuk, Korea

ABSTRACT: This paper presents a power divider that combines broadside coupling and coplanar waveguides. This structure enables tuning the coupling coefficient by changing the microstrip line width on the top and bottom surfaces and the slot spacing between the line and ground plane. The developed power divider can be easily fabricated using a single-layer structure without requiring the complex multilayer manufacturing of a printed circuit board. To verify the effectiveness of this proposed structure, simulations and measurements were performed at a center frequency of 2 GHz. The measurement results of the implemented power divider were in good agreement with simulation ones.

1. INTRODUCTION

As power dividers are the most essential passive components in modern wireless systems, their integration and minimization have been extensively researched. Most power dividers are based on quarter-wavelength transmission lines and are used in antennas, amplifiers, and mixers in wireless systems.

Power dividers using coupled transmission lines have been extensively studied. Wideband filtering power dividers with open or short-circuited stubs [1–3] as well as power dividers with multiconductor coupled lines [4, 5], compact wideband unequal in-phase structure [6], three unequal-width coupled lines [7], and filtering function [8–10] have been developed. Most coupled-line power dividers are difficult to implement using microstrip technology because the spacing between coupled lines and the line width are extremely small (on the order of several hundred micrometers).

We propose a power divider using broadside-coupled coplanar waveguides placed on the upper and lower surfaces of a printed circuit board (PCB). Unlike conventional broadside-coupled coplanar waveguide and edge-coupled power dividers, the proposed structures achieve stronger field interaction through vertical conductor coupling, allowing higher coupling coefficients, reduced circuit size, and enhanced layout flexibility. Consequently, these structures are well suited for compact and high-performance radio frequency (RF)/microwave components. The adjustable coupling mechanism enables flexible control of power distribution between multiple output paths. By varying the coupling strength through the proposed geometry, the delivered power can be dynamically adjusted according to the load demand and coupling conditions. This tunable power-distribution capability makes the proposed structure potentially useful for near-field wireless power transfer and adaptive energy routing systems [11]. The proposed divider allows the coupling coefficient to be adjusted by varying the line width and slot spacing between the line and ground plane.

Furthermore, the isolation between output ports was improved using resistors. Fig. 1 shows the three-dimensional structure of the developed power divider. The proposed device achieves the desired coupling coefficient and solves problems related to the line width and spacing of the coupled lines of existing couplers. Based on the devised structure, two-way power dividers with $1:1$ (equal) and $1:2$ (unequal) power-splitting ratios were designed at a center frequency of 2 GHz. Their performance was verified through S-parameter characteristics for power splitting, input and output matching, and isolation.

2. THEORY

Figure 2 shows a schematic of the proposed power divider using broadside-coupled coplanar waveguides. The Z-parameters of the coupled line constituting the power divider can be formulated as follows:

$$\begin{pmatrix} V_1 \\ V_2 \\ V_3 \\ V_4 \end{pmatrix} = \begin{pmatrix} Z_{11} & Z_{12} & Z_{13} & Z_{14} \\ Z_{21} & Z_{22} & Z_{23} & Z_{24} \\ Z_{31} & Z_{32} & Z_{33} & Z_{34} \\ Z_{41} & Z_{42} & Z_{43} & Z_{44} \end{pmatrix} \begin{pmatrix} I_1 \\ I_2 \\ I_3 \\ I_4 \end{pmatrix} \tag{1}$$

where the matrix elements can be expressed as follows:

$$Z_{11} = Z_{22} = Z_{33} = Z_{44} = -j\left(\frac{Z_{oe}+Z_{oo}}{2}\right)\cot\theta$$

$$Z_{12} = Z_{21} = Z_{34} = Z_{43} = -j\left(\frac{Z_{oe}-Z_{oo}}{2}\right)\cot\theta$$

$$Z_{13} = Z_{31} = Z_{24} = Z_{42} = -j\left(\frac{Z_{oe}-Z_{oo}}{2}\right)\csc\theta$$

$$Z_{14} = Z_{42} = Z_{23} = Z_{32} = -j\left(\frac{Z_{oe}+Z_{oo}}{2}\right)\csc\theta$$

The developed two-way power divider cannot be analyzed using conventional even-odd mode analysis because power-splitting ratios at output ports are different ($1:1$ and $1:$

* Corresponding author: Young Kim (youngk63@gmail.com).

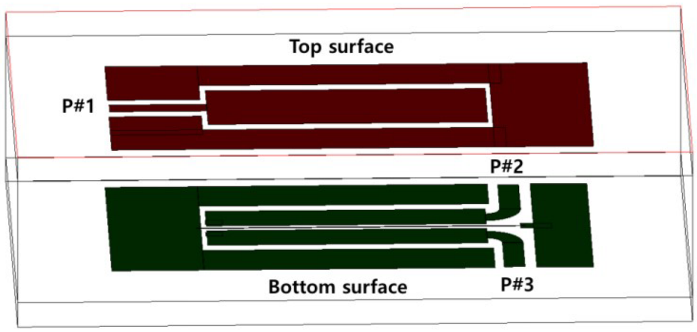

FIGURE 1. Three-dimensional configuration of the proposed power divider based on broadside-coupled coplanar waveguides.

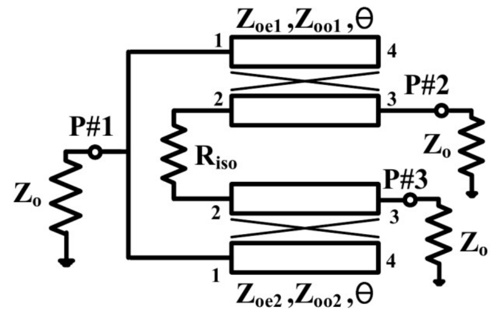

FIGURE 2. Schematic of the proposed power divider based on broadside-coupled coplanar waveguides.

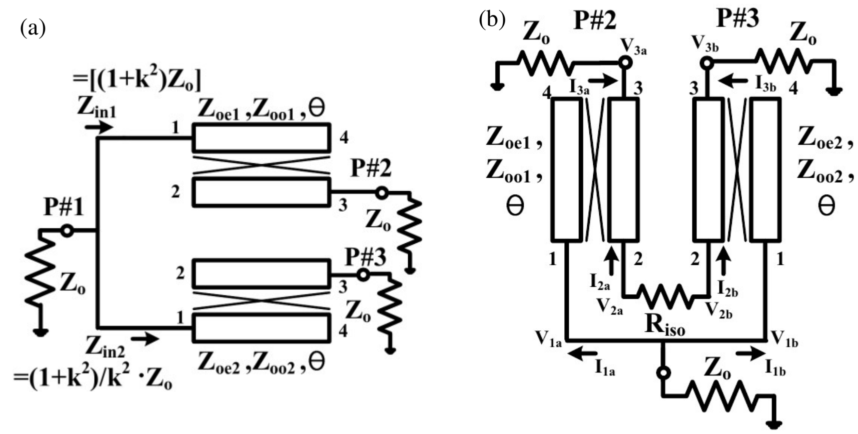

FIGURE 3. Equivalent circuits of the proposed power divider: (a) Port 1 excitation and (b) Port 2 excitation.

2). Hence, it must be analyzed using a scattering parameter method.

Figure 3(a) depicts the equivalent circuit when a signal is excited at Port 1. The power-splitting ratio between output ports is $k^2 (= P_3/P_2)$, and no current flows between output ports. In addition, Fig. 3(b) depicts the equivalent circuit when a signal is excited at Port 2. The degree of isolation between the output ports can be determined using this circuit.

Considering the equivalent circuit shown in Fig. 3(a), by applying the conditions $I_2 = 0$ and $I_4 = 0$ for the coupled-line analysis between ports 1 and 2 to Eq. (1), the equation can be rewritten as follows by converting the Z-parameters into $ABCD$ parameters [12]:

$$\begin{pmatrix} V_1 \\ I_1 \end{pmatrix} = \begin{pmatrix} A & B \\ C & D \end{pmatrix} \begin{pmatrix} V_3 \\ I_3 \end{pmatrix} \quad (2)$$

Furthermore, by converting $ABCD$-parameters in Eq. (2) into S-parameters, conditions for matching and power division between ports 1 and 2 in case of port 1 excitation were obtained as follows:

$$S_{11e2} = \frac{AZ_0 + B - CZ_{in1}Z_o - DZ_{in1}}{AZ_0 + B + CZ_{in1}Z_o + DZ_{in1}} \quad (3)$$

$$S_{21e} = \frac{2\sqrt{Z_{in1}}\sqrt{Z_o}}{AZ_0 + B + CZ_{in1}Z_o + DZ_{in1}} \quad (4)$$

$$S_{22e} = \frac{-AZ_0 + B - CZ_{in1}Z_o + DZ_{in1}}{AZ_0 + B + CZ_{in1}Z_o + DZ_{in1}} \quad (5)$$

where the parameters can be expressed as $Z_{in1} = (1+k^2) \cdot Z_o$.

S-parameters, such as S_{11e3}, S_{31e}, S_{33e}, can be derived by applying the same excitation condition used at port 1 to the network between ports 1 and 3, where the input impedance $Z_{in2} = (1+k^2)/k^2 \cdot Z_o$ is used.

The isolation between ports 2 and 3 was calculated using the equivalent circuit shown in Fig. 3(b). Based on the conditions of the equivalent circuit, namely $I_{2a} + I_{2b} = 0$, $I_4 = 0$, $V_{1a} = V_{1b} = -Z_o(I_{1a} + I_{1b})$, and $(V_{2a} - V_{2b})/R_{iso} = I_{2b} = -I_{2a}$, the relationship between ports 2 and 3 can be derived as follows:

$$\begin{pmatrix} V_{3a} \\ V_{3b} \end{pmatrix} = \begin{pmatrix} Z_{11a} & Z_{12a} \\ Z_{21a} & Z_{22a} \end{pmatrix} \begin{pmatrix} I_{3a} \\ I_{3b} \end{pmatrix} \quad (6)$$

By converting Z-parameters of Eq. (6) into S-parameters, isolation S_{21iso} between ports 2 and 3 is obtained. Using Eqs. (3)–(6), S parameters of the proposed power divider are expressed as

$$S_{11} = \frac{S_{11e2} + S_{11e3}}{2}, \; S_{21} = S_{21e}, \; S_{31} = S_{31e} \quad (7a)$$

$$S_{22} = S_{22e}, \; S_{33} = S_{33e}, \; S_{23} = S_{21iso} \quad (7b)$$

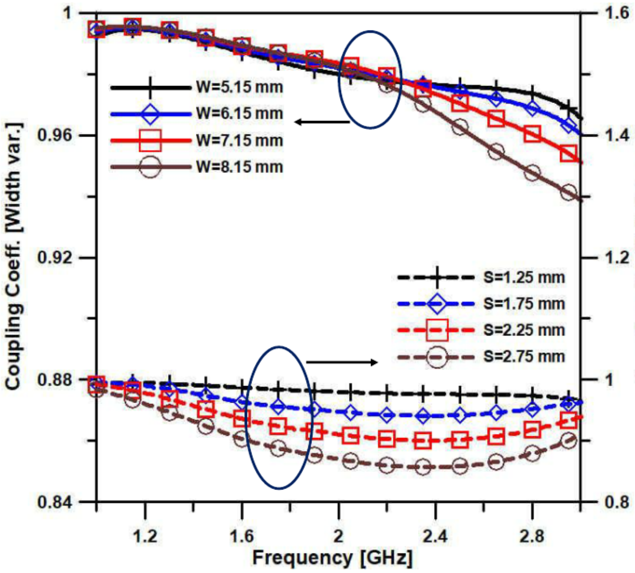

FIGURE 4. Effect of the line width and slot spacing on the coupling coefficient of the broadside-coupled coplanar waveguides.

Using Eqs. (3)–(6) and MATLAB 2015b, the even-mode impedance Z_{oe}, odd-mode impedance Z_{oo}, and isolation resistance R_{iso} of the proposed coupler were determined to satisfy S-parameter requirements in Eq. (7), including a minimum 15 dB return loss and isolation and an ideal power splitting ratio at the output ports.

The even- and odd-mode characteristic impedances (Z_{oe} and Z_{oo}) characterize electromagnetic coupling in the broadside-coupled topology. The coupling coefficient is determined by the impedance difference between the two modes, and thus precise control of these impedances is critical for designing the coupled structure. From the above considerations, even- and odd-mode characteristic impedances of the broadside-coupled topology can be expressed as [13–16]

$$Z_{oe} = Z_o \sqrt{\frac{1 + k_{coup}}{1 - k_{coup}}} \tag{8a}$$

$$Z_{oo} = Z_o \sqrt{\frac{1 - k_{coup}}{1 + k_{coup}}} \tag{8b}$$

where k_{coup} is the coupler's coupling coefficient, and Z_o is the characteristic impedance.

The coupler's structural dimensions can be determined using the obtained impedance parameters, dielectric constant, and thickness of the PCB material.

3. SIMULATION AND EXPERIMENTAL RESULTS

To validate the proposed design, two-way power dividers with dividing ratios of $1:1$ and $1:2$ were implemented considering an operating frequency of 2 GHz.

The dividers were fabricated on an RO-4350B substrate with a dielectric constant (ε_r) of 3.48, a dielectric thickness (h) of 0.762 mm, and a copper thickness (t) of 0.035 mm. Simulations

TABLE 1. Calculated dimensions of the microstrip line widths and slot gaps of the broadside-coupled coplanar waveguides of the proposed power divider (unit: mm).

1 : 1 PD	W_m	W_{FL}	W_{FM}	S_{F1}	S_{F2}
	1.6	21.8	8.1	1.2	1.2
	W_{RM1}	W_{RM2}	W_{RL}	S_{R1}	S_{R2}
	3.5	3.5	21.8	1.2	1.2
1 : 2 PD	W_m	W_{FL}	W_{FM}	S_{F1}	S_{F2}
	1.6	21.8	5.0	4.7	1.7
	W_{RM1}	W_{RM2}	W_{RL}	S_{R1}	S_{R2}
	3.8	3.5	21.8	1.1	1.7

were performed to study the S-parameter characteristics using Microwave Office (version 17).

Electrical lengths, even and odd impedances of broadside-coupled coplanar waveguides, and isolation resistance of the proposed power divider were calculated using the equations presented in Section 2.

As shown in Fig. 4, a simple parametric analysis was performed by varying the line width and slot spacing in increments of 1 mm and 0.5 mm, respectively, and calculating the corresponding coupling coefficient. The results show that the coupling coefficient changes systematically with variations in line width and slot spacing, indicating that coupling level can be effectively controlled by adjusting these geometrical parameters.

Table 1 summarizes the widths and lengths of microstrip lines and slot gaps of the broadside-coupled coplanar waveguides employed in the proposed power divider. Notably, these values were obtained through an optimization process to determine those that satisfy the desired electrical characteristics of the power divider.

Figures 5(a) and 5(b) show photographs of the front and rear views of the $1:1$ power divider, respectively. The microstrip line and slot spacing for this power divider were designed by following an optimized procedure to achieve the target power-divider characteristics. In addition, a 240 Ω isolation resistor (Murata product) was used. Figs. 5(c) and 5(d) show the measured and simulated S-parameters of the power divider with $1:1$ dividing ratio, respectively, indicating an insertion loss of $|S_{21}| = -3.34$ dB and $|S_{31}| = -3.29$ dB at an operating frequency of 2 GHz.

The amplitude imbalance between output ports is maintained within ± 0.2 dB over the frequency range of 1.0–3.0 GHz.

Furthermore, the isolation $|S_{32}|$, input return loss $|S_{11}|$, and output return losses $|S_{22}|$ and $|S_{33}|$ exceeded 20 dB at an operating frequency of 2 GHz. Considering a 15-dB return-loss criterion, the measured fractional bandwidths of $|S_{11}|$, $|S_{22}|$, and $|S_{33}|$ were 52.4%, 137%, and 137%, respectively, in 1.45–2.48, 0.50–2.69, and 0.5–2.68 GHz, respectively. Furthermore, $|S_{32}|$ was better than 15 dB in 1.49–2.29 GHz, corresponding to a fractional bandwidth of 42.3%.

Figures 6(a) and 6(b) show photographs of the front and rear views of the $1:2$ power divider, respectively. The microstrip line and slot spacing for this power divider were designed by following an optimized procedure to achieve the target power divider characteristics. In addition, a 75 Ω isolation resistor

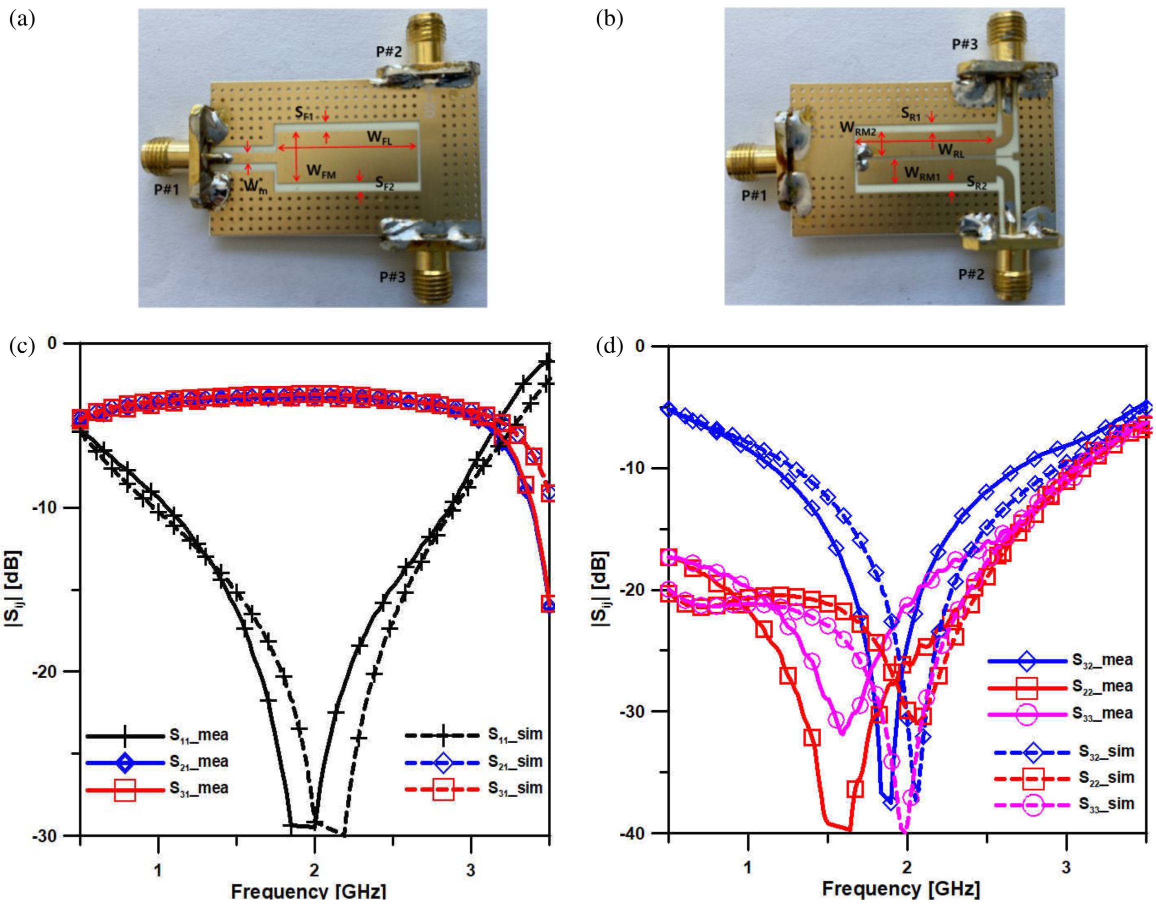

FIGURE 5. Photographs, measured and simulated S-parameter characteristics of the proposed $1:1$ two-way power divider: (a) front view, (b) rear view, and (c) $|S_{11}|$, $|S_{21}|$, and $|S_{31}|$, and (d) $|S_{32}|$, $|S_{22}|$, and $|S_{33}|$.

TABLE 2. Comparison of the proposed power divider with conventional dividers that use coupled lines.

Ref.	f_o (GHz)	IL (dB)	RL (dB)	ISO (dB)	BW (%)	Design Tech.
[1]	33	1.7	10.4	11.4	49.4/10 dB	Three coupled line
[3]	1.0	4.2	15	20	10/15 dB	coupled line BPF
[6]	7.0	0.5	12	20	114/12 dB	Three coupled line
[7]	1.5	1.0	11	14	80/11 dB	Three coupled line
[8]	2.5	1.7	17	20	58.7/15 dB	coupled line
This work (1 : 1)	2	0.3	20	20	52.4/15 dB	Broadside Coupled WG
This work (1 : 2)	2	0.5	20	20	56/15 dB	Broadside Coupled WG

(Murata product) was used. Figs. 6(c) and 6(d) show the measured and simulated S-parameters of the power divider with a $1:2$ dividing ratio, respectively, indicating an insertion loss of $|S_{21}| = -5.35$ dB and $|S_{31}| = -1.97$ dB at an operating frequency of 2 GHz.

The amplitude imbalance between output ports is maintained within ± 0.8 dB over the frequency range of 1.0–3.0 GHz. Further, the isolation $|S_{32}|$, input return loss $|S_{11}|$, and output return loss $|S_{22}|$ and $|S_{33}|$ all exceeded 20 dB at an operating frequency of 2 GHz. Considering a 15-dB return-loss criterion, the measured fractional bandwidths of $|S_{11}|$, $|S_{22}|$, and $|S_{33}|$ were 56%, 55%, and 117%, respectively, in 1.43–2.54, 1.61–2.83, and 0.74–2.84 GHz, respectively. Furthermore, $|S_{32}|$ was better than 15 dB in 1.34–2.81 GHz, corresponding to a fractional bandwidth of 70.8%.

As shown in Figs. 5 and 6, the measured results show good agreement with the simulated ones overall. The slight deviations between the simulation and measurement results are mainly attributed to fabrication tolerances and measurement uncertainties. Table 2 presents a comparison of the proposed power divider with conventional designs using coupled lines.

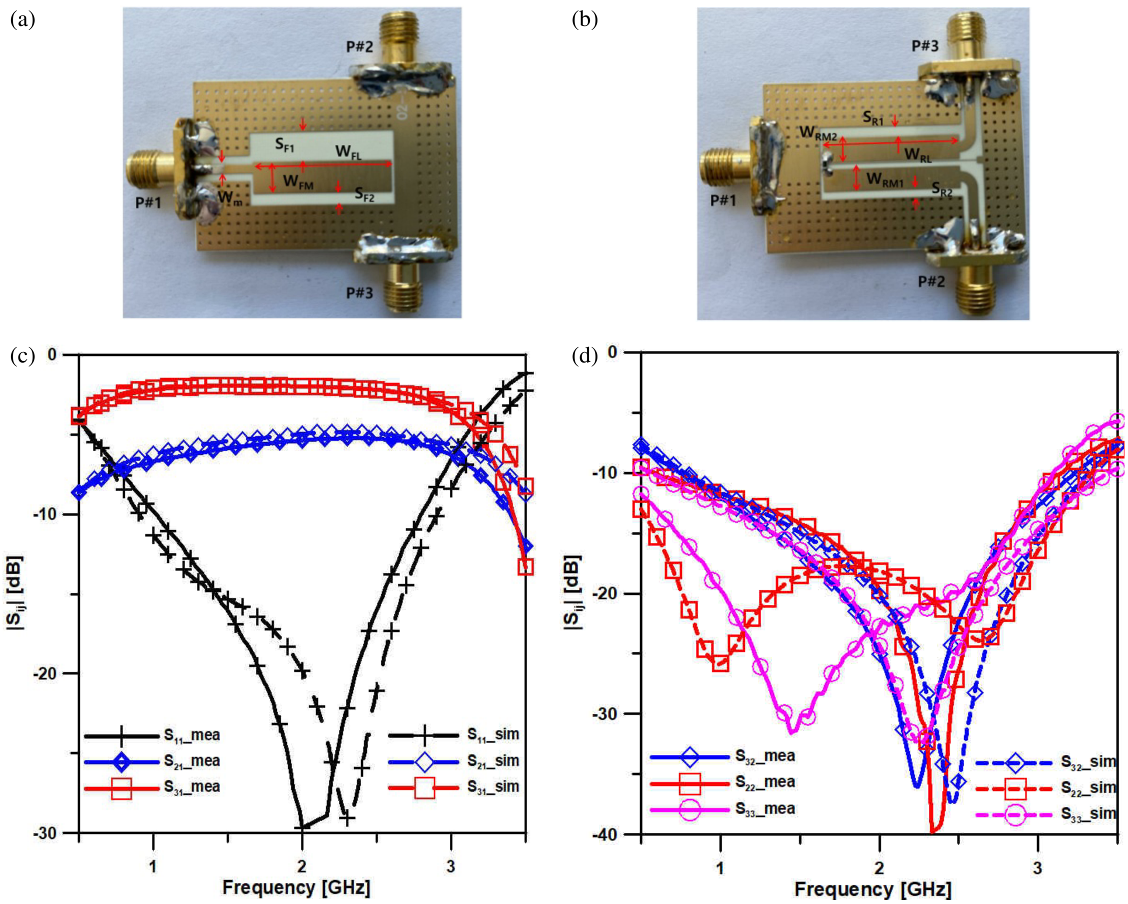

FIGURE 6. Photographs, measured and simulated S-parameter characteristics of the proposed $1:2$ two-way power divider: (a) front view, (b) rear view, and (c) $|S_{11}|$, $|S_{21}|$, and $|S_{31}|$, and (d) $|S_{32}|$, $|S_{22}|$, and $|S_{33}|$.

4. CONCLUSION

This paper presents a compact broadside-coupled coplanar waveguide power divider with an adjustable coupling mechanism. The proposed structure achieves controllable coupling characteristics while maintaining good isolation performance, and the measured results at 2 GHz show good agreement with the simulated ones, validating the proposed design. The coupling control based on geometrical parameters provides good manufacturability and practical applicability. Furthermore, the proposed topology can be extended to multi-way power dividers and integrated filtering power divider structures, making it a promising solution for compact and highly integrated RF/microwave applications. Future work will include quantitative tolerance simulations and substrate parameter sensitivity analyses to further evaluate the robustness of the proposed design and verify the engineering merits of the adjustable coupling mechanism under practical manufacturing conditions.

REFERENCES

[1] Lin, Y.-S., J.-F. Chang, and P.-T. Yeh, "Coupled-line-based millimeter-wave CMOS spiral power dividers with tapered TLs," *Analog Integrated Circuits and Signal Processing*, Vol. 109, No. 3, 625–637, 2021.

[2] Song, K., Y. Mo, and Y. Fan, "Wideband four-way filtering-response power divider with improved output isolation based on coupled lines," *IEEE Microwave and Wireless Components Letters*, Vol. 24, No. 10, 674–676, October 2014.

[3] Chen, C.-J. and Z.-C. Ho, "Design equations for a coupled-line type filtering power divider," *IEEE Microwave and Wireless Components Letters*, Vol. 27, No. 3, 257–259, 2017.

[4] Zhao, X.-B., F. Wei, P. F. Zhang, and X. W. Shi, "Mixed-mode magic-Ts and their applications on the designs of dual-band balanced out-of-phase filtering power dividers," *IEEE Transactions on Microwave Theory and Techniques*, Vol. 71, No. 9, 3896–3905, September 2023.

[5] Chiu, J.-C., J.-M. Lin, and Y.-H. Wang, "A novel planar three-way power divider," *IEEE Microwave and Wireless Components Letters*, Vol. 16, No. 8, 449–451, August 2006.

[6] Zhu, H., A. Abbosh, and L. Guo, "Ultra-wideband unequal in-phase power divider using three-line coupled structure," *Electronics Letters*, Vol. 50, No. 15, 1081–1082, 2014.

[7] Liu, H., Y. Ma, M. Guan, S. Fang, and Z. Wang, "Synthesis of miniaturized wideband four-way filtering power divider consisting of unequal-width three-coupled-lines," *International Journal of RF and Microwave Computer-Aided Engineering*, Vol. 31, No. 10, e22805, 2021.

[8] Xia, Z., J. Wang, Q.-Y. Lu, W. Wu, and J. Hong, "A wideband 90° phase shifting element applied in quadrature phase filtering power divider," *IEEE Microwave and Wireless Technology Letters*, Vol. 34, No. 2, 167–170, February 2024.

[9] Wang, D., X. Guo, and W. Wu, "Wideband unequal power divider with enhanced power dividing ratio, fully matching bandwidth, and filtering performance," *IEEE Transactions on Microwave Theory and Techniques*, Vol. 70, No. 6, 3200–3212, June 2022.

[10] Liu, Y., S. Sun, and L. Zhu, "2^n-way wideband filtering power dividers with good isolation enhanced by a modified isolation network," *IEEE Transactions on Microwave Theory and Techniques*, Vol. 70, No. 6, 3177–3187, June 2022.

[11] Guo, Z., F. Yang, H. Zhang, X. Wu, Q. Wu, K. Zhu, J. Jiang, H. Jiang, Y. Yang, Y. Li, and H. Chen, "Level pinning of anti-PT-symmetric circuits for efficient wireless power transfer," *National Science Review*, Vol. 11, No. 1, nwad172, 2024.

[12] Zysman, G. I. and A. K. Johnson, "Coupled transmission line networks in an inhomogeneous dielectric medium," *IEEE Transactions on Microwave Theory and Techniques*, Vol. 17, No. 10, 753–759, 1969.

[13] Chang, C.-P., J.-C. Chiu, H.-Y. Chiu, and Y.-H. Wang, "A 3-dB quadrature coupler using broadside-coupled coplanar waveguides," *IEEE Microwave and Wireless Components Letters*, Vol. 18, No. 3, 191–193, 2008.

[14] Tefiku, F., E. Yamashita, and J. Funada, "Novel directional couplers using broadside-coupled coplanar waveguides for double-sided printed antennas," *IEEE Transactions on Microwave Theory and Techniques*, Vol. 44, No. 2, 275–282, February 1996.

[15] Nedil, M., T. A. Denidni, and L. Talbi, "Novel Butler matrix using CPW multilayer technology," *IEEE Transactions on Microwave Theory and Techniques*, Vol. 54, No. 1, 499–507, January 2006.

[16] Sawicki, A. and K. Sachse, "Novel coupled-line conductor-backed coplanar and microstrip directional couplers for PCB and LTCC applications," *IEEE Transactions on Microwave Theory and Techniques*, Vol. 51, No. 6, 1743–1751, June 2003.